Babol University of Medical Sciences

IJMCM

International Journal of Molecular and Cellular Medicine

p-ISSN: 2251-9637 o-ISSN: 2251-9645

Cellular and Molecular Biology Research Center

P19 a Parthenin Analog Induces Cell Lineage Dependent Apoptotic and Immunomodulatory Signaling in Acute Lymphoid Leukemia Cells

Vishal Sharma[1], Samriti Dhawan[2], Ajay Kumar[3], Jagdeep Kaur[1*]

1. Department of Biotechnology, Panjab University, Chandigarh, India.

2. Department of Biotechnology, Goswami Ganesh Dutta Sanatan Dharma College, Chandigarh, India.

3. Pharmacology Division, Indian Institute of Integrative Medicine, Jammu, India.

Article type:
Original Article

Received:
2023.05.31
Revised:
2023.09.30
Accepted:
2023.09.30

ABSTRACT

Leukemia is a type of cancer that affects the blood and bone marrow. Acute lymphoid leukaemia, also known as ALL, is regarded as one of the deadliest forms of cancer. Due to the rapid increase in various cancer cases and the development of resistance in cancer cells, it is necessary to identify novel lead molecules with more potent anticancer properties. There is a growing interest in using herbal products/analogs as multi-component agents (as anticancer agents and immunomodulators) for cancer treatment. In the present investigation, an attempt has been made to explore the anticancer and immunomodulatory activity of P19, an analog of parthenin in ALL. P19 was reported to exhibit anticancer efficacy by triggering apoptotic signaling events in human leukaemia HL-60 cells by significant NO production. In contrast to this finding, ROS and NO were not required for P19-mediated apoptosis in Raji cells. The mechanism of action of P19 was observed to be cancer cell lineage dependent. P19 demonstrated very effective anticancer properties against ALL (IC_{50} 3µM). Molecular investigations revealed that P19 induced mitochondrion mediated apoptosis by Bax localization to mitochondria and enhanced cytosolic calcium in the cytoplasm. Further activation of the caspase 3, caspase 8 and PARP cleavage suggested the involvement of the caspase-mediated apoptosis. Anti-proliferative activity revealed the telomerase inhibition and cell cycle arrest in G0/G1 phase after P19 treatment. Immunomodulatory effects of the P19 revealed the enhanced INFɣ and NO production in Jurkat and THP cells. Owing to its antiproliferative and immunomodulatory potential against leukemia cells P19 can further be explored as effective therapeutics against leukemia.

Keywords: Acute lymphoid leukemia, apoptosis, immunomodulation, anticancer, Raji cells

Cite this article: Sharma V, *et al*. P19 a Parthenin Analog Induces Cell Lineage Dependent Apoptotic and Immunomodu-latory Signaling in Acute Lymphoid Leukemia Cells. *International Journal of Molecular and Cellular Medicine. 2023; 12(1):1-17.* **DOI:** 10.22088/IJMCM.BUMS.12.1.1

***Corresponding:** Jagdeep Kaur

Address: Department of Biotechnology, Panjab University, Chandigarh, India.
E-mail: jagsekhon@yahoo.com

Introduction

The term "cancer" represents a wide variety of diseases and disorders characterized by uncontrolled cell proliferation. Existing therapeutic interventions, such as surgical removal of tumor followed by chemotherapy, radiation therapy, and adjuvant therapy, each have their own advantages and disadvantages. For localized tumors, surgery and radiation are preferred treatments. Chemotherapy is preferred for metastatic tumors because it can affect cancer cells throughout the body. The agents used in chemotherapy have significant cytotoxicity or side effects on normal cells (1), which is one of its main drawbacks. A further disadvantage of chemotherapy is that cancer patients develop resistance to conventional chemotherapeutic drugs (2). Therefore, it is necessary to search and develop new compounds that provide suitable specific anti-proliferative effects that can be developed as anticancer agents. The major potential source for anticancer drug discovery is the diverse plant flora. To date, many chemotherapeutic drugs have been obtained from the plants as direct agents or as lead molecules (3). Recent trends in research have included the focus on the lid molecules, which along with the anticancer also possess the immunomodulatory nature. Recently a plant derived compound zerumbone has been shown to induce both anticancer as well as the immunomodulatory effect (4).

Parthenium hysterophorus (Family Asteraceae), an annoyingly prolific weed, also known as congress grass, is an annual herb. Plant has been used as a local remedy for the treatment of infectious and degenerative diseases (5). To enhance its bioactivity, analogs of parthenin (a major sesquiterpene lactone) were synthesized by substitutions at different reaction centers to establish a structure–activity relationship (6). A novel parthenin analog P19, was reported to demonstrate anticancer activity by activation of apoptotic signaling events through robust NO formation in human leukemia HL-60 cells (5). The pro-apoptotic activity of P19 suggested its potential use as a promising anticancer therapeutic. However, its immunomodulatory activity has not been studied to date, as the response of several anticancer drugs was observed to be different in various types of cancers (7). Therefore, an attempt has been made to investigate the anticancer potential and immunomodulatory activity of P19 against Raji, Jurkat, THP-1 cells. Our studies suggested that P19 acted as a dual agent by inducing both apoptotic as well as immunomodulatory activities.

Materials and methods

Cell culture, growth conditions and treatment

Raji cell line (B cell lymphoma), Jurkat (T cell lymphoma), THP-1 (human leukemia monocytic cell line) were procured from the National Center for Cell Science (NCCS) Pune, India. Raji cells were grown in RPMI-1640 medium containing 10% FCS (Himedia India), 100 units penicillin/100 µg streptomycin per ml medium in CO_2 incubator at 37 $^{\circ}$C with 95% humidity and 5% CO_2 gas environment. Monocytes were differentiated to macrophages using phorbol-12-myristate-13-acetate (PMA 5 ng/mL) for 48 h (8). Cells were treated with P19 dissolved in DMSO while the untreated cultures received only the vehicle (DMSO, <0.2%, v/v). All the reagents used were of analytical grade.

Cell proliferation assay

Cell proliferation was determined using 3-(4, 5-dimethylthiazol-2-yl)-2, 5-diphenyltetrazolium bromide (MTT) assay (9). Raji, Jurkat, THP-1 cells (1.0 x 10^4/well) in 96 well culture plates were treated with various

[DOI: 10.22088/IJMCM.BUMS.12.1.1]

concentrations of P19 for 48 h. The MTT formazan crystals formed were dissolved in 200 µL of DMSO, and absorbance was measured at 570 nm. The cytotoxicity of P19 was expressed as the relative viability (% of untreated or control cells).

Acridine orange/ethidium bromide staining and SEM imaging

To study the nature of P19 induced cytotoxicity, Raji cells were grown in the presence of 1.0 µM, 3.0 µM of P19 for 48 h, and were observed under fluorescence microscope (Nikon) after staining with acridine orange/ethidium bromide stain (10 µg/mL). Cells stained with the dual staining were considered as the apoptotic cells. Scanning electron microscopy (SEM) was carried out using previously defined methods (10).

Cell cycle analysis and chromosome preparations

Cell cycle analysis was carried out using propidium iodide, as described previously (9). Briefly, $1x10^6$ cells/ml after P19 (1.0 µM, 3.0 µM) treatment for 48 h were washed with chilled PBS twice. Further cells were fixed with 70% ethanol for 40 min. After that, cells were rewashed with PBS and re-suspended in 500 µL of staining solution containing propidium iodide, detergent, and RNase followed by flow cytometric analysis. Raji cells (1×10^6 cells/ml) were seeded and treated with P19 (1.0 µM, 3.0 µM) for 48 h for chromosome preparations. Both P19 treated and untreated cells were subjected to colcemid treatment (0.1µg/ml) for 2h before terminating experiment. G-banding was done using 0.005% trypsin, and chromosomes were analyzed under a light microscope. Comparative mitotic indices of the slides were calculated by considering the average values of the ratio of metaphase plate vs. the number of cells in five different areas of slides at 10X magnification.

Telomerase extract preparation and Conventional trap assay

The telomerase extract preparation and conventional trap (telomerase repeated amplification protocol) assay was carried out by the method of Mender and Shay, 2015 with minor modifications (11). Control and P19 treated cells were used for the telomerase extract preparation. Raji cells (1×10^6/ mL) with/without treatment were washed once in PBS and pelleted at 5000 rpm for 5 min at 4˚C. Further, cells were suspended in 500 µL of ice-cold washing buffer (10 mM HEPES-KOH (pH 7.5), 1.5 mM $MgCl_2$, 10 mM KCl and 1 mM dithiothreitol). Washed cells were resuspended in 200 µL of ice cold lysis buffer (10 mM Tris–HCl (pH 7.5), 1 mM $MgCl_2$, 1 mM EGTA, 0.1 mM phenylmethylsulfonyl fluoride, 5 mM β-mercaptoethanol, 1 mM dithiothreitol, 0.5% CHAPS, 10% glycerol) for 30 min. The lysate was spun at 15000 rpm for 30 min at 4˚C. The supernatant was removed, and the protein concentration in the extracts was determined by protein estimation kit (Bangalore Genie). For TRAP assay 5 µg protein was used. Assay tubes were prepared using 0.2 µg of CX primer, each extract was assayed in 50 µL of reaction mixture containing 20 mM tris-HCl (pH 7.5), 1.5 mM $MgCl_2$, 60 mM KCl, 0.005% tween 20, 1 mM EGTA, 50 µM dNTPs, and incubated at 30˚C for 30 min. PCR was carried out after heat inactivation of protein at 950C for 10 min followed by adding 0.2 µg of TS primer, and 2.5 units Taq DNA polymerase. PCR conditions were as follows: 94 ˚C for 4 min, 58˚C for 45 seconds, 72˚C for 45 seconds for 32 cycles, and 72˚C for 7 min. PCR products were fractionated by electrophoresis on 12.5 % non-denaturing polyacrylamide gels and stained with ethidium bromide for 15 min. Amplified products were visualized and analyzed using Gel doc (Bio-Rad USA).

RT-PCR and quantification of mRNA levels

[DOI: 10.22088/IJMCM.BUMS.12.1.1]

Total RNA was isolated from the treated and untreated cells after P19 treatment using the trizol reagent (An equal amount of RNA was used to synthesize cDNA after DNase treatment using the Revert Aid first-strand cDNA synthesis kit (thermo scientific). RT-PCR (Real time PCR) and semi quantitative reverse transcription PCR was carried out to check the alteration in the level of mRNA expression. Real time PCR analysis was performed in the Eppendorf real-plex system using the SYBR Green PCR Master mix (Thermo scientific USA). Real time PCR was carried out for p21, IFN-γ, IL-2, and β-actin using gene specific primers. β- actin served as an internal control. The specificity of PCR products was analyzed using the melting curve analysis, and the delta CT method was used to quantify alteration in expression (12). Expression of hTERT, hTR, TP-1, Bax and Bcl2 using the semi-quantitative reverse transcription PCR as described previously (13).

Flow Cytometry based analysis

Raji cells (1.0 x 10^6 cells/mL) were treated with P19 for 48 h and washed once in PBS. The washed cells were further, incubated with dyes 2'-7'dichlorofluorescin diacetate (DCFH-DA), 4, 5-diaminofluorescene-diacetate (DAF-2- DA), JC-1, Fluo-3 AM and subjected to reactive oxygen species (ROS), nitric oxide (NO), mitochondrial membrane potential and cytosolic calcium detection as described previously (5, 14). For fluorochrome-conjugated antibody staining, the Raji, Jurkat and THP-1 cells were washed with PBS. Further cells were fixed and permeabilized using the Cytofix/Cytoperm kit (BD, Bioscience, USA) for 20 minutes on ice. Cells were pelleted, washed with Perm Wash Buffer (BD, Bioscience, USA), and stained with fluorochrome-conjugated anti IFNγ, anti p21 antibodies (Santa Cruz Biotechnology, USA), at 40C for one hour. Finally, cells were washed again and resuspended in the Perm Wash Buffer for flow cytometry analysis. Flow cytometric analysis was performed on a BD FACS Canto II (BD Biosciences, USA) for a maximum cell count of ten thousand and analyzed using BD FACSDiva software.

Western blot analysis

Cells were harvested, and the cell pellet was washed with cold PBS. Cells were lysed in lysis buffer (20 mM Tris HCl (pH 7.5), 150 mM NaCl, 1% NP-40, 1 mM ethylene glycol-bis (β-amino ethyl ether)-tetra acetic acid, 1 mM EDTA, 50 mM NaF, 1 mM β-glycerophosphate, 2.5 mM sodium pyrophosphate, 1 mM orthovanadate, 1mM protease inhibitor cocktail, 1 mM phenylmethylsulfonyl fluoride PMSF and protein content in the supernatant was determined by protein estimation kit (Bangalore Genie). Equal amount of cell lysate from both treated and untreated was resolved on 10% SDS-PAGE followed by transfer onto a polyvinylidene difluoride (PVDF) membrane. Membranes were blocked with 5% skim milk in PBS and then probed with anti TP53 (1:1000), anti caspase 3 (1:1000), anti caspase 8 (1:1000) anti PARP (1:1000) anti NFκB (1:1000) antibodies (Sigma USA). Horseradish peroxidase-conjugated secondary antibodies were used to detect immune-reactive bands using 3, 3'-Diaminobenzidine as substrate.

β- Galactosidase staining and in gel activity assay

Beta-galactosidase staining was performed as described previously (15). Briefly, Raji cells were treated with P19 for 48 h, followed by washing in PBS. After this cells were fixed in 2% formaldehyde/0.2% glutaraldehyde and rewashed with PBS at 37°C. For staining cells from the previous step were incubated with fresh senescence-associated β-Gal stain solution. For in gel activity assay of catalase and superoxide dismutase (SOD) total cell lysate (equivalent to one unit of either catalase or SOD activity) was subjected to

[DOI: 10.22088/IJMCM.BUMS.12.1.1]

native polyacrylamide gel electrophoresis at room temperature. Afterwards, gels were rinsed with 200 ml water and then stained for either catalase or SOD activity using the protocols described previously (16).

Results

P19 induced anti proliferative and apoptotic effect on leukemic cells

P19 inhibited Raji cells in a dose dependent manner with IC_{50} of 3.0 ± 0.60 (µM) (Figure 1A). The effect of P19 on THP-1 and Jurkat cells was studied as these cells were further used to find out the immunomodulatory effects. P19 decreased the proliferation of Jurkat and THP-1 cells with an IC_{50} of 1.0 ± 0.3 (µM) and 3.0 ± 0.4 (µM), respectively (Figure 1A). To confirm the nature of cytotoxicity, Raji cells were treated with P19 (1.0 µM, 3.0µM) and subjected to DNA laddering assay, acridine orange/ethidium bromide staining. In comparison with untreated cells, P19 treated Raji cells revealed extensive DNA fragmentation (Figure 1B). Furthermore, acridine orange/ethidium bromide double staining displayed large green nuclei with intact membranes in untreated cells. However, P19 (3.0 µM) treated Raji cells revealed a significant decrease in large green nuclei and exhibited signs of apoptotic cells indicated by orange and red fluorescent (Figure 1C). Further morphological analysis of P19 treated Raji cells using SEM revealed characteristic membrane blebbing while untreated cells revealed intact membrane indicating the cytotoxic effect of P19 (Figure 1D). Raji cells treated with P19 were subjected to propidium iodide and observed under the fluorescent microscope. P19 treated cells at 3.0 µM showed a significant condensation of the nucleus, while the untreated cells showed an intact nucleus (Figure 1E). Collectively these results indicated that Raji cells underwent apoptosis after treatment with P19.

P19 caused cell cycle arrest in G_0/G_1 phase and did not contribute to genomic instability

Cell cycle analysis revealed that P19 (1.0 µM, 3.0 µM) treatment to Raji cells induced cell cycle arrest in G0/G1 phase. P19 treated Raji cells revealed increased count from 54 % to 72 % in G0/G1 phase in comparison to control (untreated cells), while a significant decrease in S phase and G2/M was observed suggesting G0/G1 phase arrest in Raji cells (Figure 2A, B). Tofurther investigate the impact of P19 on genomic stability, chromosome preparation was carried out after P19 (1.0 µM, 3.0 µM) treatment. P19 treated Raji cells did not show any chromosome breakage as compared to control cells (Figure 2C). The comparative mitotic index of control slides was found to be 0.35, while for P19 treated slides, 0.17 was observed. Collectively these observations suggested that P19 induced apoptosis in Raji cells was independent of genomic instability.

P19 mediated apoptosis independent of NO and ROS in Raji cells.

Since P19 was documented previously to induce ROS mediated apoptosis in HL-60 cells, we evaluated this molecule for its potential to induce ROS and NO in Raji cells (5). P19 treated HL-60 cells were considered as positive control (Figure 3A, B). We did not observe any significant variation in ROS and NO content in P19 (1.0 µM, 3.0 µM) treated Raji cells, whereas P19 treated HL-60 cells showed a marked increase in ROS and NO (Figure 3A-B). Further to rule out the role of catalase and SOD in P19 treated Raji cells, in-gel activity was accessed. No significant change in the activity of SOD and catalase was observed (Figure 3C). The activity profile correlated with the transcription profile of these genes. Semi quantitative reverse transcription PCR analysis revealed no significant change in the expression of these genes (Figure

[DOI: 10.22088/IJMCM.BUMS.12.1.1]

3D). Collectively these results suggested that P19 did not affect the antioxidant system and P19 mediated apoptosis was independent of ROS and NO induction in Raji cells.

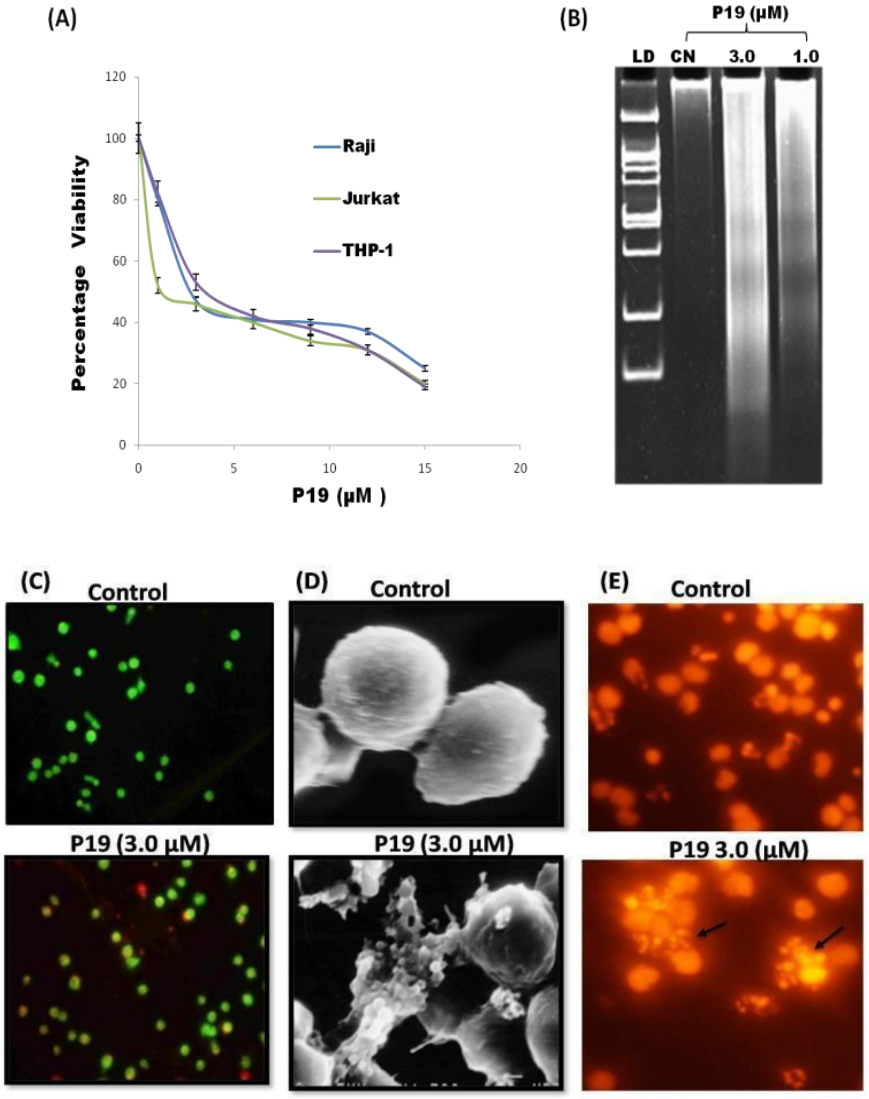

Fig.1. P19 treatment induced cytotoxic and apoptotic effect in cancer cells.
(A) The cytotoxic effect of P19 on Raji, Jurkat and THP-1 cells was assessed by MTT assay. Cells were treated with increasing concentration of P19 (0-15 µM) for 48 h. Cytotoxicity was expressed as percentage viability as compared to control. Data are presented as the mean ± S.D. of three similar experiments (B) DNA laddering assay after treatment of Raji cells with P19 (1.0 µM, 3.0µM). P19 treated cells showed enhanced DNA fragmentation as compared to control. (C) Acridine orange/ethidium bromide stained images of Raji cells after P19 treatment (3.0 µM). Early and late apoptosis was depicted by orange and red color respectively, which was visualized by fluorescence microscope (D) SEM images of morphological changes in Raji cells after treatment with P19 (3.0 µM). P19 treated Raji cells revealed a typical membrane blebbing pattern, while untreated cells revealed intact membrane (E) Images of propidium iodide stained Raji cells treated with P19 (3.0 µM). P19 treatment-induced nucleus condensation/fragmentation in Raji cells as compared to control cells. Arrow indicated the fragmented nucleus in P19 treated Raji cells. Untreated cells were considered as control. Data are representative from one of three similar experiments.

[DOI: 10.22088/IJMCM.BUMS.12.1.1]

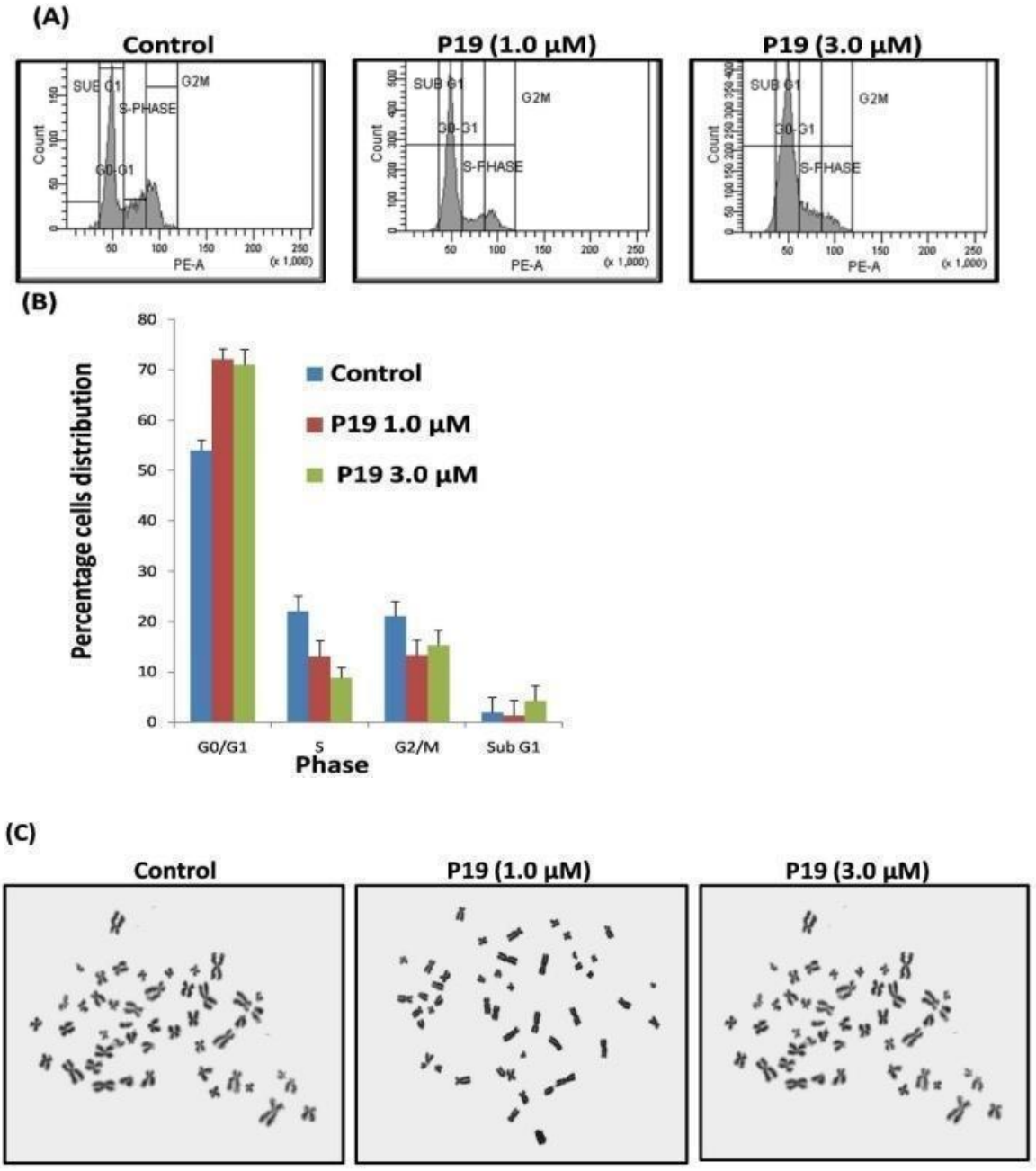

Fig.2. P19 treatment induced G_0/G_1 phase cell cycle arrest and did not induce genomic instability in Raji cells.
(A)Cell cycle analysis of Raji cells by flow cytometry after P19 treatment. Raji cells were treated with P19 (1.0 µM, 3.0 µM) for 48 h and cell cycle distribution was determined after propidium iodide DNA staining. The area parameter histogram was used to determine the percentage of cells in G0/G1, S, G2/M phase. Ten thousand events were counted per tube (B) Bar graphs of cell cycle distribution shown as the percentage change in cells distribution in P19 treated and control cells. Data are presented as the mean ± S.D. of three similar experiments. (C) Metaphase plates showing chromosome after P19 treatment. Raji cells were treated with different concentrations of P19(1.0 µM, 3.0 µM) for 48 h, and chromosome preparation was carried out by subjecting cells to mitotic arrest using colcemid for 2h before the termination of the experiment. P19 treated Raji cells did not show any breakage in chromosome arms. Untreated cells were considered as control. Data are representative from one of three similar experiments.

[DOI: 10.22088/IJMCM.BUMS.12.1.1]

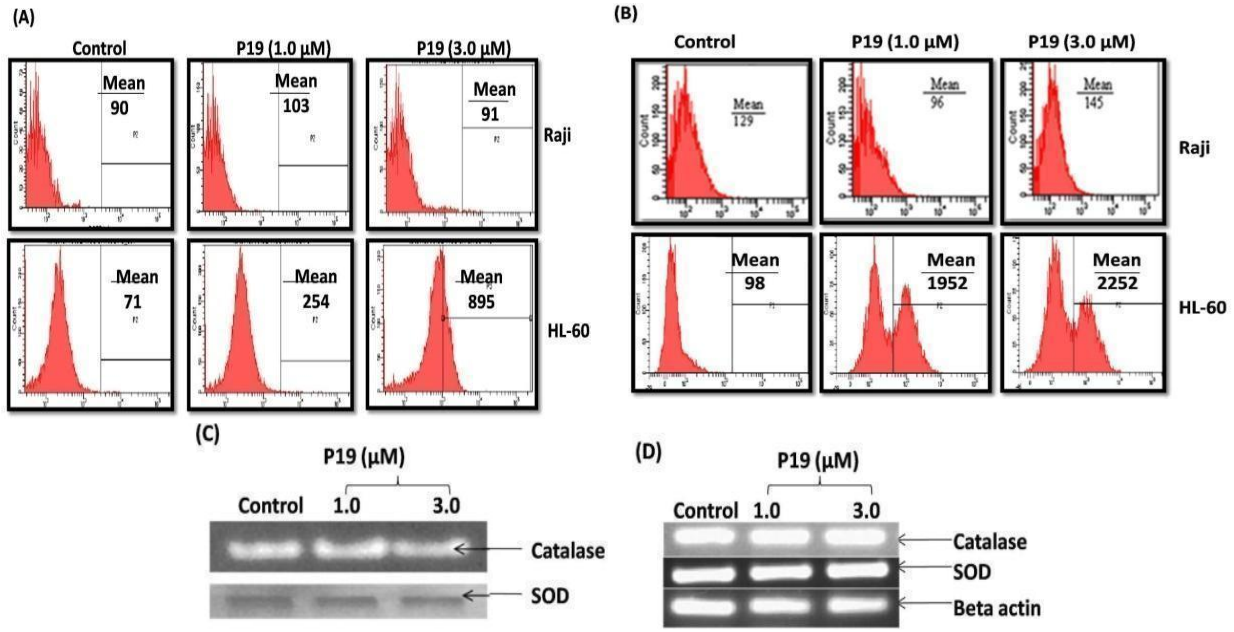

Fig.3. P19 induced ROS and NO independent apoptosis in the Raji cell line.
(A) FACS analysis histogram of DCFH-DA stained Raji and HL-60 cells after treatment with P19 (1.0 µM, 3.0 µM) for 48 h. Mean values indicate oxidative stress inside the cells. HL-60 cells were considered as a positive control for ROS induction after P19 treatment. P19 treatment did not induce ROS in Raji cells (B) FACS analysis histogram of DAF-2-DA stained Raji and HL -60 cells treated with different concentrations of P19 (1.0 µM, 3.0 µM) for 48 h followed by DAF-2-DA staining and flow cytometric analysis. Mean values indicate NO stress inside the cells. HL-60 cells after P19 treatment were considered as a positive control for NO induction after P19 treatment. P19 treatment did not induce ROS in Raji cells (C) In-gel activity assay for catalase, SOD in P19 treated (1.0 µM, 3.0 µM) Raji cells. The total cell lysate was resolved on native 12.5% PAGE, and bands were developed after incubating in the developing medium as described in material and method. (D) Semi quantitative reverse transcription PCR analysis of SOD and catalase gene expression in Raji cells after P19 treatment. Agarose gel electrophoresis of PCR amplified SOD and catalase genes products. Raji cells treatment with P19 did not alter the catalase, SOD activity and expression. Beta-actin served as an internal control. Five thousand events were counted per tube for flow cytometric analysis. Data are representative from one of three similar experiments.

P19 enhanced cytosolic calcium level and induced mitochondrion mediated apoptosis.

The calcium ion is an important secondary messenger in controlling cell signaling and cell death (17). Enhanced cytosolic calcium level was documented previously linked to mitochondrial and caspase mediated apoptosis induction (18). Therefore, evaluation of cytosolic calcium was carried out after treatment with the P19. Results revealed the enhanced cytosolic calcium after P19 treatment in Raji cells as compared to control (Figure 4A). Simultaneously treatment of Raji cells with P19 resulted in upregulation of Bax and downregulation of antiapoptotic Bcl2 protein (Figure 4C). Both cytosolic calcium and Bax translocation have been documented to induce mitochondrial mediated apoptosis (19). Therefore, to determine the translocation of Bax from the cytosol to mitochondria, cytosolic and mitochondrial fractions from P19 treated Raji and control cells were subjected to western blot analysis. A significant increase in the level of Bax in the mitochondrial fraction was concomitant with a decreased level of Bax expression in cytosolic fraction in P19 treated cells as compared to control (Figure 4D). Simultaneously an alteration in mitochondrial membrane potential and a significant increase in the cytosolic cytochrome c were observed after P19 treatment as

[DOI: 10.22088/IJMCM.BUMS.12.1.1]

compared to control (Figure 4E-F). These studies suggested that Bax could lead to mitochondrial membrane potential loss, and which can result in release of cytochrome c from the mitochondrion. Together these observations indicated that P19 treated Raji cells underwent apoptosis in the mitochondrial mediated pathway.

The induction of caspases and poly-ADP ribose polymerase (PARP) has been considered as a critical feature of apoptosis (20). Therefore, after monitoring the enhanced expression of cytosolic cytochrome c, we analyzed the expression of caspase 3. Western blot analysis showed the enhanced level of cleaved caspase 3 in P19 treated Raji cells while an intact band of caspase 3 was observed in control cells (Figure 4H). Further caspase 3 and caspase 8 activation was found linked with PARP cleavage. PARP cleavage leads to the activation of various endonucleases that cleave DNA and results in DNA fragmentation. The higher level of cleaved PARP was observed after P19 treatment in Raji cells. Collectively all these observations suggested that P19 induced caspase mediated apoptosis in Raji cells.

P19 induced TP53 upregulation and inhibition of telomerase activity

TP53 participates in the cellular response to various stress conditions and plays a significant role in apoptosis induction (21). Therefore, we evaluated the status of TP53 in P19 induced apoptosis. When Raji cells were treated with P19 (1.0 µM and 3.0 µM) a significant upregulation in TP53 protein was observed as compared to control (Figure 5A). TP53 has been documented to activate the expression of p21 (22). Therefore, we further analyzed the expression of p21 at both mRNA level (RT PCR) and protein level (flow cytometry) (Figure 5B). It was observed that P19 treatment upregulated the p21 mRNA by more than 3 fold in Raji cells as compared to control. At the same time, flow cytometric analysis after staining with fluorochrome conjugated anti p21 antibody revealed nearly 2fold enhanced expression of p21 after P19 (3.0 µM) treatment (Figure 5B-C). These results suggested that P19 induced TP53, which in turn increased the p21 expression resulting in cell cycle arrest and apoptosis induction.

Inhibition of the telomerase activity is the key feature of the anticancer drug discovery (23). Keeping this in mind we evaluated the effect of P19 on telomerase inhibition. TRAP assay revealed that telomerase activity was inhibited in a concentration dependent manner as indicated by a decrease in laddering pattern with an increase in the concentration of P19 (Figure 5E). Further, Raji cells treated with P19 showed the most β-galactosidase staining as compared to untreated cells, which suggested that P19 mediated inhibition of telomerase lead to senescence induction in Raji cells (Figure 5D). To determine the mechanism of action of P19 on telomerase, we evaluated the expression of three telomerase components, hTERT, hTR, and TP-1, using the semi quantitative reverse transcription PCR as described in the material and method section. The results revealed no significant change in the expression of any subunit as compared to control. These results suggested that P19 inhibited the telomerase by targeting it at protein level (Figure 5F).

P19 modulates the expression of various cytokines

Since targeting cancer with a dual strategy (anticancer and immunomodulatory) could be a more effective treatment, we evaluated the immunomodulatory activity of P19. Interleukin 2 (IL-2) and interferon-gamma (IFNγ) were selected for our investigation, since these molecules have been documented to play a significant role in anticancer activities (24). The expression of cytokines (IL-2 and IFNɣ) was analyzed by RT-PCR. A significant upregulation in the expression of cytokine IFNɣ(7 fold), IL-2(6 fold) was observed in Jurkat cells

[DOI: 10.22088/IJMCM.BUMS.12.1.1]

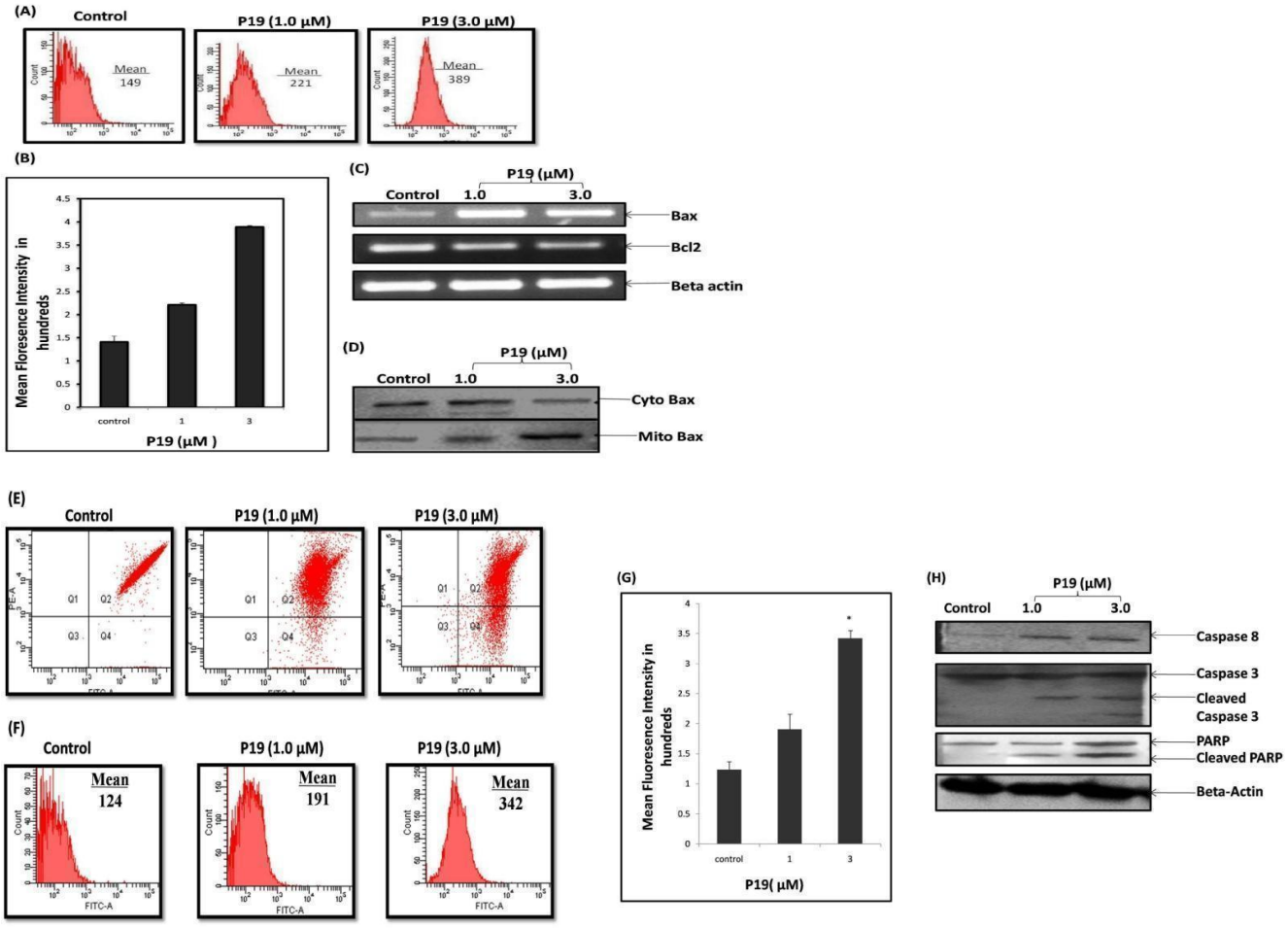

Fig.4. P19 induced enhanced cytosolic calcium level, mitochondrial dysfunction, and caspase mediated apoptosis. (A) FACS analysis histograms of Flou-3AM stained Raji cells after P19 (1.0 µM, 3.0 µM) treatment for 48 h. Mean value indicated the cytosolic calcium level inside the cells. (B) Bar graph showing the change in cytosolic calcium level after P19 treatment expressed as mean fluorescence intensity. P19 treatment enhanced cytosolic calcium level in Raji cells. Data are presented as the mean ± S.D. of three similar experiments (C) Semi quantitative reverse transcription PCR analysis showing the expression of Bax and Bcl2 genes in P19(1.0 µM, 3.0 µM) treated Raji cells. Agarose gel electrophoresis of PCR amplified Bax and Bcl2 gene products. Beta-actin was taken as an internal control. (D) Western blot signals of Bax distribution in the mitochondrion and cytosolic fractions after P19 treatment in Raji cells. Raji cells were treated with indicated concentrations of P19 followed by immunoblot analysis of Bax in the mitochondrion, cytosolic fractions. Enhanced expression of Bax was observed in mitochondrial fraction as compared to control (E) FACS analysis histograms of JC-1 stained Raji cells after treatment with P19 (1.0 µM, 3.0 µM) for 48 h. P19 treatment induced the loss of mitochondrial membrane potential in Raji cells (F) FACS profile of fluorochrome conjugated anti cytochrome c antibody stained Raji cells treated with P19 (1.0 µM and 3.0 µM). (G) Bar graph showing the change in cytosolic cytochrome c expression after P19 treatment expressed as mean fluorescence intensity. Data are presented as the mean ± S.D. of three similar experiments. P19 treatment induced enhanced cytosolic cytochrome c expression in Raji cells (H) Western blot signals of caspase 8 expression, caspase 3 and PARP cleavage, after treatment of Raji cells with P19 at indicated concentrations for 48 h. Total cell lysates were resolved on 10% SDS-PAGE and subjected to immunoblot analysis using anti caspase 8, anti caspase 3 and anti PARP antibodies. P19 treatment induced caspase 8 expression, caspase 3 and PARP cleavage in Raji cells. Beta-actin was considered as an internal control. Raji cells without treatment were taken as control. Five thousand events were counted per tube for flow cytometric analysis * represents the statistically significant ($P<0.05$) difference between control and P19 treated cells. Data are representative from one of three similar experiments.

[DOI: 10.22088/IJMCM.BUMS.12.1.1]

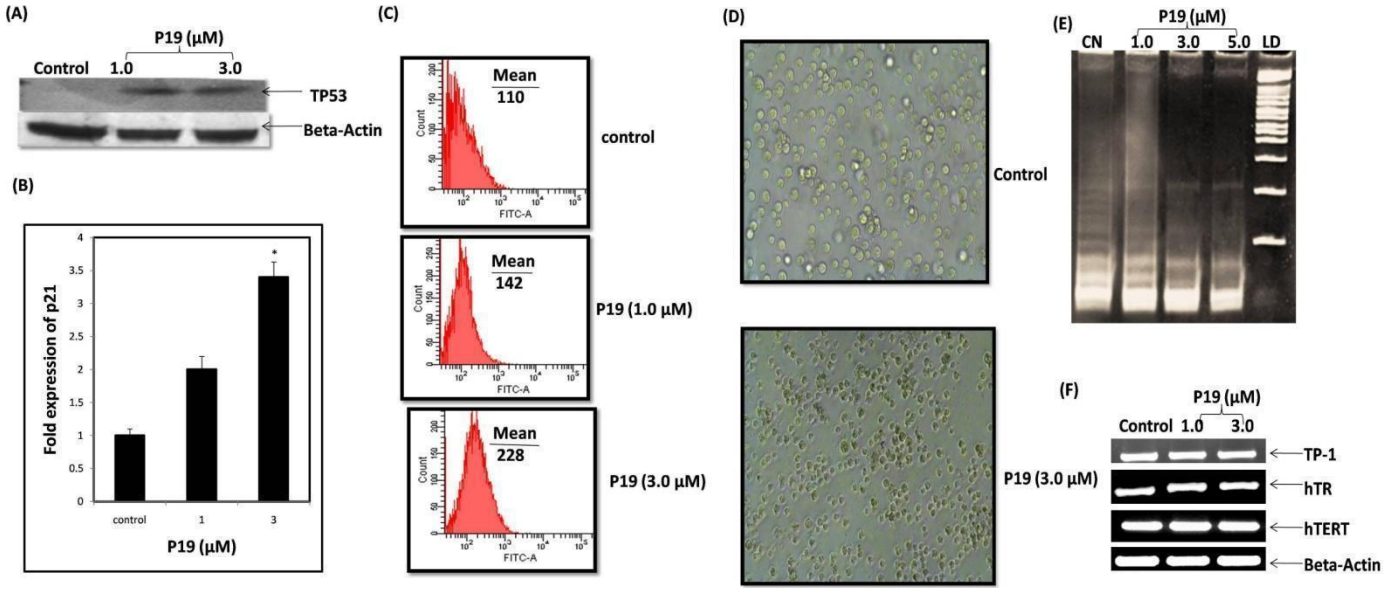

Fig.5. P19 treatment induced TP53, p21 expression, and inhibition of telomerase activity in Raji cells.
(A) Western blot signals of TP53 in P19 treated Raji cells. Raji cells were treated with different concentrations of P19 (1.0 µM 3.0 µM) for 48 h, and total cell lysate was resolved on 10% SDS page and subject to immunoblot analysis using antiTP53 antibodies. P19 treatment induced TP53 protein expression in Raji cells. Beta-actin was considered as internal control. (B) RT PCR analysis to quantify the relative change in p21 gene expression. Total RNA was isolated, and RT PCR was carried out using gene-specific primers. Beta-actin was considered as internal control. The specificity of reaction products was analyzed using melting curve analysis. Data are presented as the mean ± S.D. of three similar experiments(C) Flow cytometric profile of anti p21 stained Raji cells treated with P19 (1.0 µM 3.0 µM). The mean value depicted the level of p21 in Raji cells expressed as mean fluorescence intensity. P19 treatment induced p21 mRNA and protein expression in Raji cells (D) β-galactosidase stained P19 treated Raji cells and control cells at the indicated concentrations (E) TRAP assay showing inhibition of telomerase activity by P19 in Raji cell. Telomerase activity in Raji cells was analyzed by the TRAP assay after treatment of Raji cells with P19 (1.0 µM to 5.0 µM). Amplified PCR products were resolved on 12.5% non-denaturing polyacrylamide gel. (F) Semi-quantitative reverse transcription PCR analysis for change in expression of telomerase subunit genes (TP-1, hTR, hTERT) after P19 treatment in Raji cells. No significant change in TP-1, hTR, hTERT mRNA was observed after P19 treatment. Beta-actin was considered as an internal control,* represents the statistically significant (P<0.05) difference between control and P19 treated cells. Data are representative from one of three similar experiments.

after P19 treatment (Figure 6A). Similarly, in THP-1 cells (differentiated to macrophage cells), P19 treatment resulted in upregulation of IFNɣ (5 fold), IL-2 (3 fold) (Figure 6B) in comparison to untreated cells. The results were further validated by staining of Jurkat and THP-1 cells with fluorochrome conjugated anti IFNɣ antibody (Figure 6C). P19 enhanced the expression of IFNɣ in Jurkat and THP-1 cells. P19 could induce Jurkat cells more efficiently to produce IFNɣ at a very low concentration (0.5-1.0 µM). These results suggested that P19 could modulate the immune system by enhancing the expression of major cytokines, including IFNɣ. Because NO production is one of the critical mechanisms in the immune response we analyzed the level of NO in Jurkat and THP-1 cells (25). Contrary to Raji cells, the treatment of Jurkat and THP-1 cells with P19 resulted in enhanced NO production (Figure 6E). As the NO production is dependent on iNOS (inducible nitric oxide synthase), the effect of P19 on the expression of iNOS was also checked. The induction in NO production was further supported by enhanced iNOS expression in Jurkat (Figure 6G,I) and THP-1 cells (Figure 6H, J). Further, to analyze the mechanism behind the simultaneous expression of

[DOI: 10.22088/IJMCM.BUMS.12.1.1]

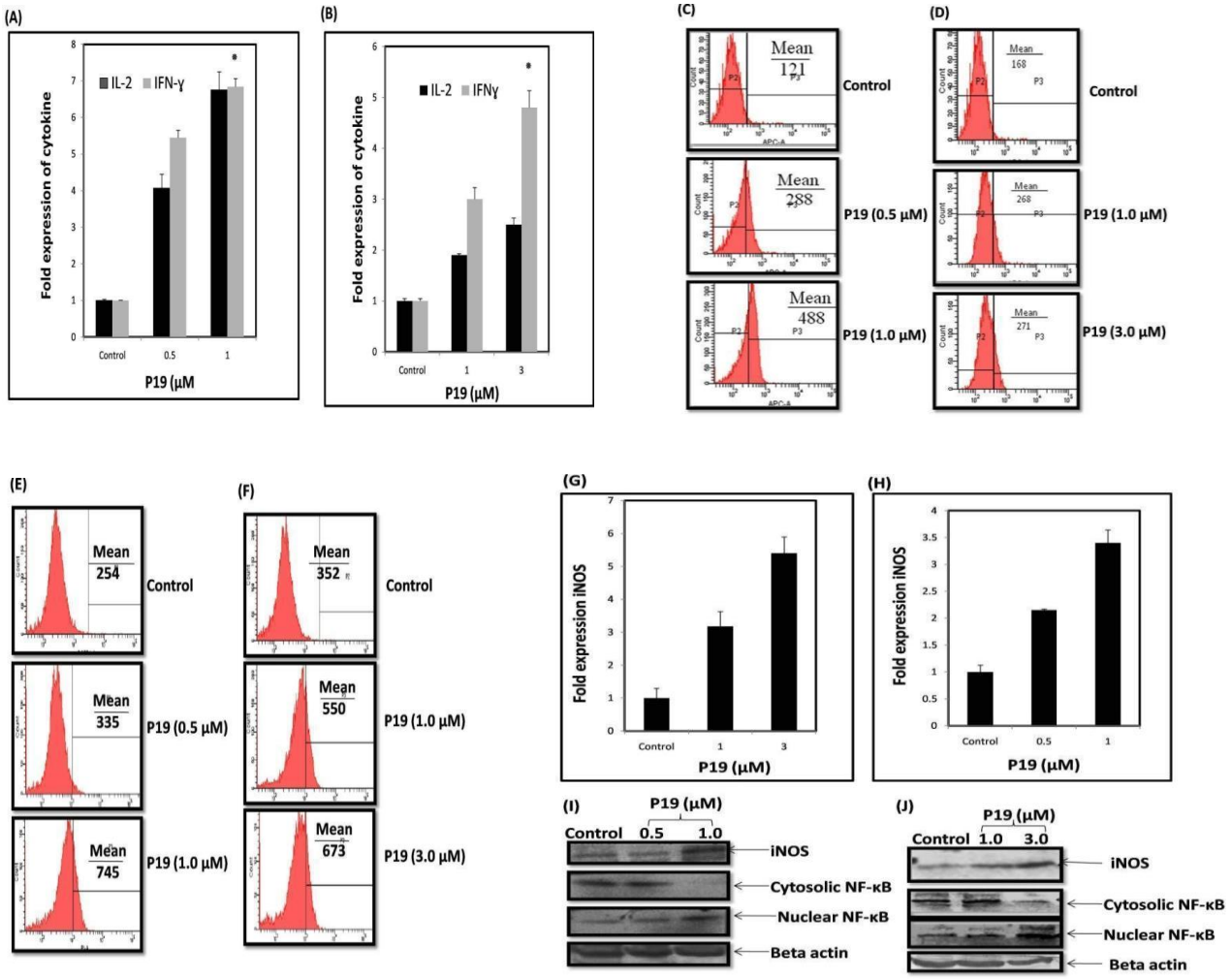

Fig.6. P19 treatment enhanced the expression of different cytokines (IL-2 and IFNγ), iNOS, NO production and nuclear localization of NF-κB in Jurkat cells (A, C, E, H, I) and THP-1 (B, D, F, G, J).

(A) RT PCR analysis of change in cytokine gene (IL-2, IFNγ) expression after P19 (0.5 μM -1.0 μM) treatment in Jurkat cells for 48 h. (B) RT PCR analysis of change in cytokine gene (IL-2, IFNγ) expression after P19 (1.0 μM 3.0 μM) in THP-1 cells for 48 h. Jurkat and THP-1 cell lines were treated with different concentrations of P19 (below and at IC_{50}). Total RNA was isolated and RT PCR was carried out to analyze the change in expression of different cytokines using gene-specific primers. The specificity of reaction products was analyzed by melting curve analysis. Beta-actin was considered as an internal control. Data are presented as the mean ± S.D. of three similar experiments (C, D). FACS analysis histograms of anti IFNγ antibody stained Jurkat cells (C) and THP-1 cells (D) after P19 treatment. Jurkat and THP-1 cells were treated with indicated concentrations of P19 (below and at IC_{50}) and analyzed using flow cytometry after staining with fluorochrome-conjugated anti IFNγ antibody. Mean values represent the change in expression of IFNγ expressed as mean fluorescence intensity. Five thousand events were counted per tube. (E, F) FACS analysis histograms of NO estimation in Jurkat (E) and THP-1 (F) cells after P19 treatment. Jurkat and THP-1 cells were treated with indicated concentrations of P19 (below and at IC_{50}) for 48 h followed by DAF-2-DA staining and flow cytometric analysis. Mean values indicate NO stress inside the cells. (G, H) RT-PCR analysis for iNOS expression in Jurkat, (G), and THP-1 (H) cells after treatment with P19. (I, J) Western blot analysis of iNOS expression and nuclear localization of NF-κB in Jurkat (I) and THP-1(J) cells after P19 treatment at indicated concentrations. Total cell lysates or cell lysate after cytosolic and nuclear fractionation were resolved on 10% SDS-PAGE for immunoblot analysis of iNOS and NF-κB expression. P19 treatment induced enhanced iNOS expression and nuclear localization in Jurkat and THP-1 cells. Untreated cells were considered as control. * represents the statistically significant ($P<0.05$) difference between control and P19 treated cells. Data are representative from one of three similar experiments.

[DOI: 10.22088/IJMCM.BUMS.12.1.1]

various cytokines and NO induction, the nuclear localization of nuclear factor-kappa-B (NF-κB) was analyzed by western blot analysis in Jurkat and THP-1 cell lines. NF-κB is the key transcription factor involved in the activation and transcription of various cytokines along with NO induction by the iNOS mediated pathway (26). NF-κB was translocated to the nucleus after treatment with P19. It was observed that P19 caused cleavage of NF-κB and enhanced the nuclear localization of NF-κB in Jurkat and THP-1 (Figure 6I, J) cells. These studies suggested that P19 induced NF-κB mediated immunomodulation.

Discussion

New anticancer agents are needed to treat cancer more effectively and stop the emergence of drug resistance. Because of their low toxicity, scientists expressed an interest in plants as a source of plant-based drugs for cancer. The anticancer potential of several compounds extracted from plants has been identified (27,28). These compounds generally target the genes involved in the progression of cell cycle/apoptosis (29). In the present investigation anticancer potential of P19 was evaluated against Raji cells. P19 demonstrated a significant cytotoxic effect against Raji cells. The IC_F of P19 for Raji cells is slightly higher than the previously reported for HL-60 cells (5). DNA fragmentation assay and microscopic analysis pointed towards apoptosis as the mechanism for observed cytotoxicity with P19 compound. Beside the induction of cytotoxic action in Raji cells, the compound induced the anti-proliferative effect as revealed by the cell cycle arrest in G0/G1 phase and was independent of genomic stability or chromosomal damage. Some of the plants derived anticancer compounds such as curcumin formerly documented to induce genomic instability in Raji cells (9). However, there was no change in chromosome integrity in P19 treated Raji cells.

P19 was reported to induce apoptosis through robust NO production in HL-60 cells (5). Contrary to this observation, P19 mediated apoptosis in Raji cells was independent of NO and ROS induction. Moreover, no change in activity and gene expression of catalase and SOD ruled out the involvement of antioxidant defense mechanisms. The mechanism of P19 was observed to be cancer cell lineage dependent. These studies are supported by the previous studies where many natural compounds like Alternol works in a cell lineage dependent manner and follow different mechanisms in different cell lineages (30). As reported earlier, P19 induced translocation of Bax to mitochondria, disruption of mitochondrial function with concurrent loss of mitochondrial membrane potential, release of cytochrome c to the cytosol, activate caspase cascade in HL-60 cells (5). In concordance with these studies, Raji cells treatment with P19 revealed enhanced cytosolic calcium and translocation of Bax from cytosolic fraction to mitochondrial fraction. While the expression of Bcl2 decreased. Previously also, many anticancer drugs involved in cancer treatment or under trial are very well known to induce Bax mediated apoptotic effects in malignant cells (31). Bax is a pro apoptotic protein and documented to alter mitochondrial membrane potential (32). Similarly altered mitochondrial membrane potential as well as enhanced cytosolic cytochrome c level was reported after P19 treatment in Raji cells. Recent studies both in vitro and in vivo have revealed that various natural compounds exert their anticancer mechanism by mitochondrial mediated pathways. Similarly, our study also suggested that P19 treatment of Raji cells resulted in mitochondrial dysfunction and enhanced cytochrome c levels. Inductions of caspase and PARP cleavage have been considered as downstream executioners of enhanced cytochrome c levels (33). In the same way P19 treatment also showed caspase 3, caspase 8 induction and PARP cleavage. All these

[DOI: 10.22088/IJMCM.BUMS.12.1.1]

studies together revealed mitochondria and caspase mediated apoptosis induction in Raji cells after P19 treatment.

Tumor suppression is the main function of p53 protein, which is encoded by the TP53 gene on human chromosome 17, it is activated in response to DNA damage. P53 promotes the synthesis of pro-apoptotic genes in the nucleus by increasing p21 expression and can also target the telomerase (34). Many potential strategies to target the cancer are documented to exert anticancer effects by restoring the TP53 mediated pathways (35). Therefore, an attempt was made to study the expression pattern of TP53 and its downstream effector p21 after treatment with test compounds. P19 could induce the expression of TP53 and p21 in Raji cells. This might be a reason for cell cycle arrest in the G0/G1 phase. It is demonstrated that in Raji cells, telomerase activity was suppressed by P19 in a concentration manner. Previous studies have indicated that telomerase expression is associated with cell immortalization and tumorigenesis, which made telomerase an attractive target for cancer therapy (36). Especially in leukemia where over-expression of telomerase has been reported earlier (37). Recent study also suggested that anticancer effects of drugs can be enhanced by inhibiting telomerase activity (38). Few Parthenin compounds have also been documented to suppress the telomerase activity in cervical cancer cell lines (6). Our studies also suggested that P19 inhibited the telomerase activity in a concentration dependent manner, while no change in the expression of telomerase subunit was observed. These studies were r supported by the activation of senescence in Raji cells after P19 treatment, as demonstrated by β-galactosidase assay. Studies with P19 on Raji cells collectively suggested that P19 could lead to the cell cycle arrest and inhibit the telomerase activity.

The immune system's natural capacity to detect and destroy abnormal cells plays a vital role in cancer prevention. Cytotoxic drug treatment and tumor microenvironment conditions induce several alternative modes for cancer cell death. However, certain forms of drug-induced cell death are much more useful than others because of their ability to activate potent anticancer immune responses (39). Immunotherapy is another type of cancer treatment involving modulation of the patient's immune system for targeting cancer cells. Some of the anticancer drugs (such as taxol) were reported to exert an additive effect in the treatment of cancer by the modulation of the host defense system (40). Among the immunomodulatory effects, NO production by immune cells is a crucial event. It has been reported that NO derived from macrophages, kupffer cells, natural killer cells, and endothelial cells participates in tumoricidal activity against many types of tumors (41). Along with NO, cytokines, IL-2 and IFNɣ play a significant role in fighting against the cancer cells. Among these, IL-2 has been considered as the first effective immunotherapy against the tumors (42). Dunn et al., 2006 have shown that immunotherapy with IFNɣ in cancer patients improved the lives of cancer patients (43, 44). Therefore, the study was extended to reveal the immunotherapeutic potential of P19. Upon treatment with P19 Jurkat and differentiated macrophages lead to significant production of IFNɣ, IL-2. Macrophages and Jurkat cells generated a large amount of NO, whereas in the case of Raji cells no ROS or NO production was observed. The enhanced level of iNOS suggested an iNOS mediated pathway involvement in NO production. Recent research has shown that cytokines (IL-2, and IFNɣ) and iNOS can be induced by NF-κB mediated pathway (45, 46). The treatment of Jurkat and THP-1 cells with the P19 followed by nuclear localization of NF-κB suggested the involvement of NF-κB in the induction of cytokines and iNOS, resulting in the production of NO. These macrophages, in turn, play an important role in immune

[DOI: 10.22088/IJMCM.BUMS.12.1.1]

surveillance against tumors during their development by presenting tumor antigen to cytotoxic T cells and releasing tumoricidal substances like cytokines and nitric oxide. Previously, many natural plant products like garlic and curcumin have also been shown to modulate the immune system (47, 48). A comparison of P19 to other molecules suggested that P19 is a novel anticancer molecule that possesses cytotoxic properties and immuno-modulatory functions even at very low dose kinetics.

P19 inhibited cancer cell proliferation. It inhibited telomerase activity of these cells and induced TP53, which in turn increased the p21 expression resulting in cell cycle arrest and apoptosis induction. P19 also induced the expression of IL-2, IFNɣ in macrophages, and T cells via activation of NF-kB, resulting in the induction of iNOS and the NO. In this study, we showed that in addition to cytotoxic activity, P19 exhibited immunomodulatory activity at a relatively low dose. These observations suggested that P19 could be a promising anticancer agent to consider for more research on animal tumor models and even human clinical trials.

References

1. Schirrmacher V. From chemotherapy to biological therapy: A review of novel concepts to reduce the side effects of systemic cancer treatment (Review). Int J Oncol 2019;54:407-19.

2. Huang CY, Ju DT, Chang CF, et al. A review on the effects of current chemotherapy drugs and natural agents in treating non-small cell lung cancer. Biomedicine (Taipei) 2017;7:23.

3. Seca AML, Pinto D. Plant Secondary Metabolites as Anticancer Agents: Successes in Clinical Trials and Therapeutic Application. Int J Mol Sci 2018;19.

4. Keong YS, Alitheen NB, Mustafa S, et al. Immunomodulatory effects of zerumbone isolated from roots of Zingiber zerumbet. Pak J Pharm Sci 2010;23:75-82.

5. Kumar A, Malik F, Bhushan S, et al. A novel parthenin analog exhibits anti-cancer activity: activation of apoptotic signaling events through robust NO formation in human leukemia HL-60 cells. Chem Biol Interact 2011;193:204-15.

6. Shah BA, Kaur R, Gupta P, et al. Structure-activity relationship (SAR) of parthenin analogues with pro-apoptotic activity: Development of novel anti-cancer leads. Bioorg Med Chem Lett 2009;19:4394-8.

7. Akhdar H, Legendre C, Aninat C, et al. Anticancer drug metabolism: chemotherapy resistance and new therapeutic approaches. Top Drug Metab 2012:138-70.

8. Park EK, Jung HS, Yang HI, et al. Optimized THP-1 differentiation is required for the detection of responses to weak stimuli. Inflamm Res 2007;56:45-50.

9. Sharma V, Jha AK, Kumar A, et al. Curcumin-Mediated Reversal of p15 Gene Promoter Methylation: Implication in Anti-Neoplastic Action against Acute Lymphoid Leukaemia Cell Line. Folia Biol (Praha) 2015;61:81-9.

10. Wang G, Huang W, He H, et al. Growth inhibition and apoptosis-inducing effect on human cancer cells by RCE-4, a spirostanol saponin derivative from natural medicines. Int J Mol Med 2013;31:219-24.

11. Mender I, Shay JW. Telomerase Repeated Amplification Protocol (TRAP). Bio Protoc 2015;5.

12. Livak KJ, Schmittgen TD. Analysis of relative gene expression data using real-time quantitative PCR and the 2(-Delta Delta C(T)) Method. Methods 2001;25:402-8.

13. Zhang RG, Zhang RP, Wang XW, et al. Effects of cisplatin on telomerase activity and telomere length in BEL-7404 human hepatoma cells. Cell Res 2002;12:55-62.

[DOI: 10.22088/IJMCM.BUMS.12.1.1]

14. Bhushan S, Kumar A, Malik F, et al. A triterpenediol from Boswellia serrata induces apoptosis through both the intrinsic and extrinsic apoptotic pathways in human leukemia HL-60 cells. Apoptosis 2007;12:1911-26.
15. Dimri GP, Lee X, Basile G, et al. A biomarker that identifies senescent human cells in culture and in aging skin in vivo. Proc Natl Acad Sci U S A 1995;92:9363-7.
16. Weydert CJ, Cullen JJ. Measurement of superoxide dismutase, catalase and glutathione peroxidase in cultured cells and tissue. Nat Protoc 2010;5:51-66.
17. Cerella C, Diederich M, Ghibelli L. The dual role of calcium as messenger and stressor in cell damage, death, and survival. Int J Cell Biol 2010;2010:546163.
18. Chovancova B, Hudecova S, Lencesova L, et al. Melatonin-Induced Changes in Cytosolic Calcium Might be Responsible for Apoptosis Induction in Tumour Cells. Cell Physiol Biochem 2017;44:763-77.
19. Sharma V, Kaur R, Bhatnagar A, et al. Low-pH-induced apoptosis: role of endoplasmic reticulum stress-induced calcium permeability and mitochondria-dependent signaling. Cell Stress Chaperones 2015;20:431-40.
20. Brauns SC, Dealtry G, Milne P, et al. Caspase-3 activation and induction of PARP cleavage by cyclic dipeptide cyclo(Phe-Pro) in HT-29 cells. Anticancer Res 2005;25:4197-202.
21. Chen J. The Cell-Cycle Arrest and Apoptotic Functions of p53 in Tumor Initiation and Progression. Cold Spring Harb Perspect Med 2016;6:a026104.
22. Gu Z, Jiang J, Tan W, et al. p53/p21 Pathway involved in mediating cellular senescence of bone marrow-derived mesenchymal stem cells from systemic lupus erythematosus patients. Clin Dev Immunol 2013;2013:134243.
23. Cunningham AP, Love WK, Zhang RW, et al. Telomerase inhibition in cancer therapeutics: molecular-based approaches. Curr Med Chem 2006;13:2875-88.
24. Floros T, Tarhini AA. Anticancer Cytokines: Biology and Clinical Effects of Interferon-alpha2, Interleukin (IL)-2, IL-15, IL-21, and IL-12. Semin Oncol 2015;42:539-48.
25. Wink DA, Hines HB, Cheng RY, et al. Nitric oxide and redox mechanisms in the immune response. J Leukoc Biol 2011;89: 873-91.
26. Amoah-Apraku B, Chandler LJ, Harrison JK, et al. NF-kappa B and transcriptional control of renal epithelial-inducible nitric oxide synthase. Kidney Int 1995;48:674-82.
27. Zhou Y, Zhang Ah, Sun H, et al. Plant-derived natural products as leads to antitumor drugs. Plant Sci Today 2014;1:46-61.
28. Pan L, Chai HB, Kinghorn AD. Discovery of new anticancer agents from higher plants. Front Biosci (Schol Ed) 2012;4:142-56.
29. Alimbetov D, Askarova S, Umbayev B, et al. Pharmacological Targeting of Cell Cycle, Apoptotic and Cell Adhesion Signaling Pathways Implicated in Chemoresistance of Cancer Cells. Int J Mol Sci 2018;19.
30. Yeung ED, Morrison A, Plumeri D, et al. Alternol exerts prostate-selective antitumor effects through modulations of the AMPK signaling pathway. The Prostate 2012;72:165-72.
31. Yuan B, Imai M, Kikuchi H, et al. Cytocidal effects of polyphenolic compounds, alone or in combination with, anticancer drugs against cancer cells: potential future application of the combinatory therapy. Apoptosis and Medicine: IntechOpen; 2012.
32. Zhao G, Zhu Y, Eno CO, et al. Activation of the proapoptotic Bcl-2 protein Bax by a small molecule induces tumor cell apoptosis. Mol Cell Biol 2014;34:1198-207.
33. De Martino L, Marfé G, Longo M, et al. Bid cleavage, cytochrome c release and caspase activation in canine coronavirus-induced apoptosis. Vet Microbiol 2010;141:36-45.

[DOI: 10.22088/IJMCM.BUMS.12.1.1]

34. Chen RJ, Wu PH, Ho CT, et al. P53-dependent downregulation of hTERT protein expression and telomerase activity induces senescence in lung cancer cells as a result of pterostilbene treatment. Cell Death Dis 2017;8:e2985.
35. Qin JJ, Li X, Hunt C, et al. Natural products targeting the p53-MDM2 pathway and mutant p53: recent advances and implications in cancer medicine. Genes Dis 2018;5:204-19.
36. Shay JW, Keith WN. Targeting telomerase for cancer therapeutics. Br J Cancer 2008;98:677-83.
37. Wang L, Xiao H, Zhang X, et al. The role of telomeres and telomerase in hematologic malignancies and hematopoietic stem cell transplantation. J Hematol Oncol 2014;7:61.
38. Cerone MA, Londono-Vallejo JA, Autexier C. Telomerase inhibition enhances the response to anticancer drug treatment in human breast cancer cells. Mol Cancer Ther 2006;5:1669-75.
39. Hahn T, Polanczyk MJ, Borodovsky A, et al. Use of anti-cancer drugs, mitocans, to enhance the immune responses against tumors. Curr Pharm Biotechnol 2013;14:357-76.
40. Panis C, Lemos LG, Victorino VJ, et al. Immunological effects of taxol and adryamicin in breast cancer patients. Cancer Immunol Immunother 2012;61:481-8.
41. Li LM, Kilbourn RG, Adams J, et al. Role of nitric oxide in lysis of tumor cells by cytokine-activated endothelial cells. Cancer Res 1991;51:2531-5.
42. Rosenberg SA. IL-2: the first effective immunotherapy for human cancer. J Immunol 2014;192:5451-8.
43. Dunn GP, Koebel CM, Schreiber RD. Interferons, immunity and cancer immunoediting. Nat Rev Immunol 2006;6:836-48.
44. Beatty GL, Paterson Y. Regulation of tumor growth by IFN-gamma in cancer immunotherapy. Immunol Res 2001;24:201-10.
45. Dey P, Panga V, Raghunathan S. A Cytokine Signalling Network for the Regulation of Inducible Nitric Oxide Synthase Expression in Rheumatoid Arthritis. PLoS One 2016;11:e0161306.
46. Lorsbach RB, Murphy WJ, Lowenstein CJ, et al. Expression of the nitric oxide synthase gene in mouse macrophages activated for tumor cell killing. Molecular basis for the synergy between interferon-gamma and lipopolysaccharide. J Biol Chem 1993;268:1908-13.
47. Catanzaro M, Corsini E, Rosini M, et al. Immunomodulators Inspired by Nature: A Review on Curcumin and Echinacea. Molecules 2018;23.
48. Arreola R, Quintero-Fabian S, Lopez-Roa RI, et al. Immunomodulation and anti-inflammatory effects of garlic compounds. J Immunol Res 2015;2015:401630.

[DOI: 10.22088/IJMCM.BUMS.12.1.1]